New Diamond and Frontier Carbon Technology
Vol. 16, No. 3 2006
MYU Tokyo

NDFCT 511

Synthesis of Carbon Nanotubes by Arc-Discharge Method

Yoshinori Ando* and Xinluo Zhao

21st Century COE Program 'Nano Factory', Department of Materials Science and Engineering, Meijo University, Shiogamaguchi 1-501, Tenpaku-ku, Nagoya 468-8502, Japan

(Received 16 March 2006, accepted 11 April 2006)

Key words: multiwalled carbon nanotubes, arc discharge, hydrogen arc, carbon nanowire, Raman spectra, single-walled carbon nanotubes

In this review, we focus on the synthesis of multiwalled and single-walled carbon nanotubes (MWNTs and SWNTs, respectively) by an arc discharge method. MWNTs can be obtained in the cathode deposit of the dc arc discharge of pure graphite rods. Ambient gas plays an important role, and pure hydrogen gas is the best gas for obtaining high-crystallinity MWNTs. A thin innermost tube of less than 0.4 nm diameter and a carbon nanowire including a carbon chain can be produced by a hydrogen-ambient dc arc discharge method. The Raman spectra of MWNTs are important because radial breathing modes with frequencies higher than 300 cm^{-1} and a new Raman band near 1850 cm^{-1} appear. In the case of SWNT synthesis by an arc discharge method, the incorporation of catalytic metal particles in a graphite anode is necessary, and SWNTs are obtained as soot in an evaporation chamber. By an arc-plasma-jet method wherein two electrodes are placed at a sharp angle, the yield of soot including SWNTs is increased by decreasing the amount of cathode deposit. In particular, the arc evaporation of a graphite rod with a pure Fe catalyst in a gas mixture (hydrogen + inert gas) is effective for obtaining macroscopic SWNT nets. The purification of the SWNTs nets by heat and hydrochloric acid treatments is easy.

1. Introduction

The arc-plasma evaporation of pure graphite rods led to the discovery of carbon nanotubes (CNTs) by Iijima.[1] The arc apparatus used was the same as that for the production of ultrafine SiC particles[2] by a gas evaporation method.[3] CNTs were obtained in the cathode deposit prepared by a dc arc discharge method in rarefied He gas.[1,4] The first specimen in which Iijima found CNTs was prepared by one of the present authors (Y. A.).

*Corresponding author: e-mail: yando@ccmfs.meijo-u.ac.jp

The cathode deposit was obtained as a byproduct of fullerene production[5] by the arc discharge evaporation of pure graphite rods. The arc discharge method for producing fullerene is a modification of Krätschmer's method[6] for evaporating two carbon rods in contact by ac resistance heating. By separating the contact and applying a dc arc discharge between two pure carbon rods, the evaporation of the anode carbon realized the mass production of fullerene.[5,7] This arc evaporation of carbon electrodes produced a deposit on the cathode, which included multiwalled carbon nanotubes (MWNTs).[1] The smallest innermost tube of MWNTs was obtained by this method in pure hydrogen gas ambient.[8,9]

By a method similar to that for MWNT production, but using graphite rods including catalytic metals, single-walled carbon nanotubes (SWNTs) were discovered[10,11] in chamber soot (not in cathode deposit). The mass production of SWNTs was also realized using the same catalytic arc discharge method.[12,13] Macroscopic nets of SWNTs were obtained by a similar arc discharge method[14] in a gas mixture (hydrogen + inert gas) using a pure Fe catalyst. Some reviews[15,16] on the production of MWNTs and SWNTs by arc discharge evaporation are given by the present authors.

2. Production of CNTs by Arc Discharge Method

A schematic diagram of the arc-evaporation apparatus for producing CNTs,[17] which is a vacuum chamber, is shown in Fig. 1. Two graphite electrodes are installed vertically, and the distance between the two rod tips is maintained in the range of 1–2 mm. After the

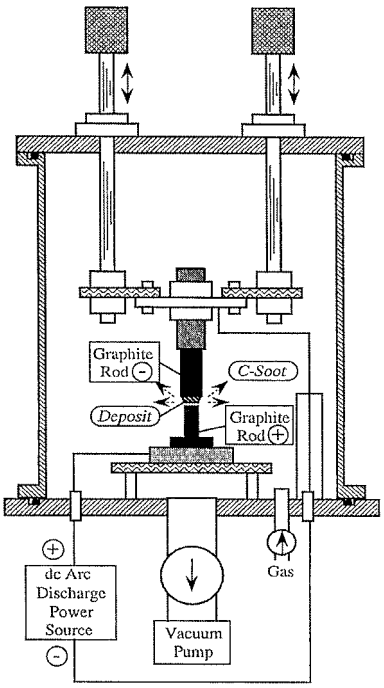

Fig. 1. Schematic diagram of apparatus[17] for preparing CNTs.

evacuation of the chamber by a diffusion pump, rarefied ambient gas is introduced. When a dc arc discharge is applied between the two graphite rods, the anode is consumed, and fullerene is formed in the chamber soot.[5] Then, part of the evaporated anode carbon is deposited on the top of the cathode; this is called the 'cathode deposit'. An optical image of a section of the cathode deposit is shown[4] in Fig. 2. On the top of cathode A, a deposit having columnar texture B is formed, and its thickness *d* is approximately 6 mm. Part C is the top of the cathode deposit facing the anode.

Iijima observed samples obtained from region B in Fig. 2 by transmission electron microscopy (TEM) and found MWNTs.[1] Typical high-resolution TEM (HRTEM) micrographs of MWNTs published in a previous paper[1] are shown in Fig. 3. Symmetrical parallel

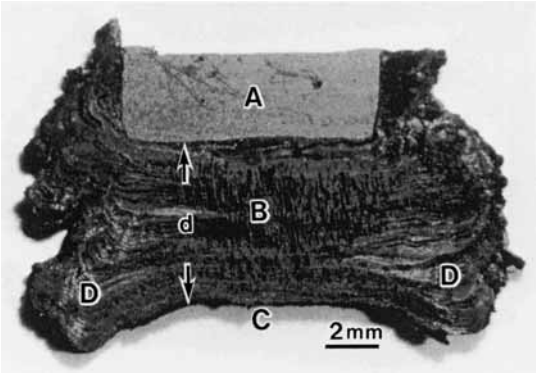

Fig. 2. Optical image of section of cathode deposit grown by dc arc discharge method in He (1.33×10^4 Pa) after 8-min evaporation.[4] Region A is the tip of the cathode. Region B has a columnar texture and contains MWNTs. Region C is the top of the cathode deposit facing the anode. Region D shows hard graphite layers. *d* is the thickness of the deposit.

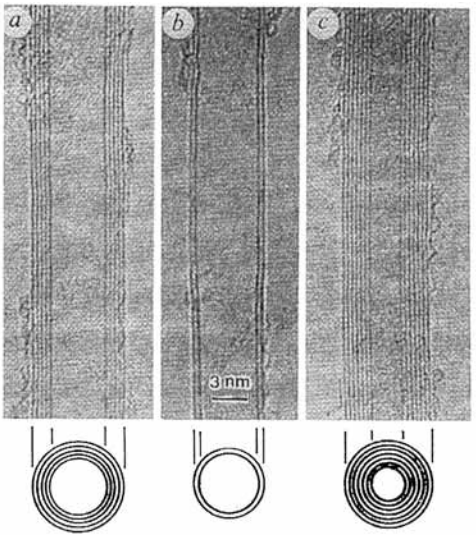

Fig. 3. HRTEM micrographs of first MWNTs discovered by Iijima.[1] Symmetrical parallel lines correspond to the projections of graphene sheets coaxially arranged with a constant spacing of 0.34 nm.

lines around the central line correspond to the projections of graphene sheets coaxially arranged with a constant spacing of 0.34 nm. The central part with no contrast is the real projection of the tubes.

The mass production of MWNTs by this dc arc discharge evaporation was first achieved by Ebbesen and Ajayan.[18] After discovering MWNTs, one could easily recognize them by scanning electron microscopy (SEM),[15] as shown in Fig. 4. In the SEM micrograph, a number of fibrous MWNTs and nanoparticles can be observed. This cathode deposit was produced by dc arc evaporation in He gas at 2.66×10^4 Pa. To clarify the effect of ambient gas,[19] dc arc evaporation was performed in He, Ar and CH_4 gases at 1.33×10^4 Pa. As observed in Fig. 5, CH_4 gas is considered the best among these three gases in producing

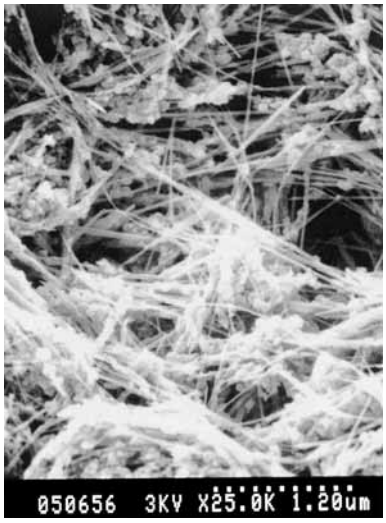

Fig. 4. SEM micrograph of MWNTs and nanoparticles produced in He (2.66×10^4 Pa).[15]

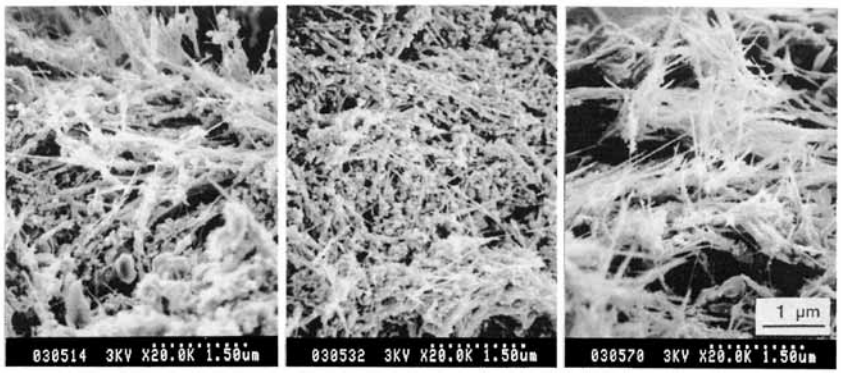

(a) He (b) Ar (c) CH_4

Fig. 5. SEM micrographs of MWNTs produced in different ambient gases[19] at pressure of 1.33×10^4 Pa. (a) He, (b) Ar and (c) CH_4.

fibrous MWNTs.[19] This is the crucial difference between this case and the case of fullerene, because fullerene could not be produced by dc arc evaporation in gas including hydrogen atoms.[20]

To clarify the efficiency of CH_4 gas, ambient CH_4 gas was mass-analyzed after dc arc evaporation.[21] After the arc discharge, H_2 and C_2H_2 gases were produced, confirming the thermal decomposition reaction[21]

$$2CH_4 \rightarrow 3H_2 + C_2H_2 . \quad (1)$$

The chamber pressure measurement showed a twofold increase in pressure after the arc evaporation. These results suggest the effectiveness of dc arc discharge in pure H_2 gas or C_2H_2 gas. In fact, C_2H_2 showed results similar to those of CH_4, but H_2 showed marked results, as described in the following section.

3. Hydrogen Ambient Arc Discharge

3.1 *Products of hydrogen arc discharge evaporation*

Arc discharge evaporation between two pure graphite rods was carried out in pure H_2 gas.[22,23] A top view[24] of the cathode deposit produced by hydrogen arc evaporation for 2 min is shown in Fig. 6. The top surface is composed of three regions: a central black region (A), a surrounding silver-gray region (B), and a very thin outer region (C). The thickness of the deposit is approximately 2 mm in regions A and B, but that in region C is less than 0.2 mm. When observing the deposit surface by SEM, MWNTs are observed in region A, and 'carbon rose' is observed[22] in region C. This carbon rose is an aggregate of petal-like graphene sheets and is composed of several parallel graphene sheet layers, the thinnest sheet layer consisting of only two graphene sheets. Similar structure materials were obtained by

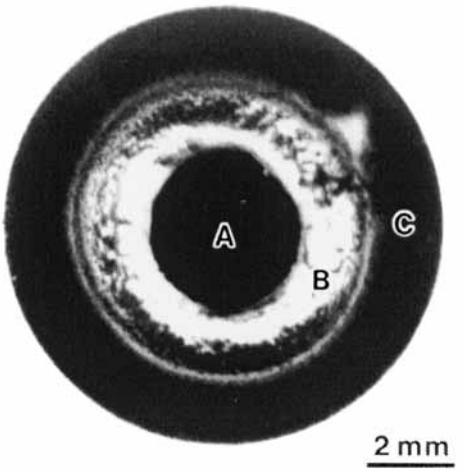

Fig. 6. Top view of cathode surface[24] deposited by pure hydrogen dc arc discharge evaporation for 2 min. Regions A and B are both 2 mm thick, and region C is very thin. MWNTs exist in region A, whereas petal-like graphite sheets exist in region C.

other methods; they are now called 'carbon nanowalls' by other groups.[25,26]

An example of the SEM micrographs of MWNTs observed in region A in Fig. 6 is shown in Fig. 7(a). In this micrograph, long and fine fibrous MWNTs and a few coexisting carbon nanoparticles can be observed, which are fairly different from MWNTs produced by the He arc discharge method shown in Fig. 4. Because the observed coexisting carbon nanoparticles are very few in number, the purification of MWNTs is easy. Purification[27] was performed by exposing an as-grown sample to infrared radiation in air at 500°C for 30 min; the resulting SEM micrograph is shown in Fig. 7(b). Almost all the nanoparticles were removed, and very long MWNTs and their bundles were observed. From the SEM micrograph, it was confirmed that purification is successfully carried out at the thickness of 100 μm from the deposit surface. The purified cathode deposit appears like a sponge of 10 mm^2 surface area and 0.1 mm thickness and can easily be handled using tweezers. The X-ray diffraction, Raman spectra[28] and magnetic properties[29] of the purified sponge were studied.

The electrical conductivity of individually purified MWNTs was measured using a two-probe method.[30,31] As shown in Fig. 8, the temperature dependence of electrical resistance was measured.[32] Curve a in Fig. 8 was obtained from a single MWNT, and arrows show the direction of temperature change. The temperature dependence shows the semiconducting characteristic of MWNTs. On the other hand, curve b was obtained from a bundle of MWNTs and shows a metallic characteristic. Field emission measurements of a spongy bulk of purified MWNTs were also carried out.[32] A practically desirable field emission current density of 1 mA/cm^2 was achieved only at an anode voltage of 580 V and a field of 1.2 V/μm.

3.2 *Thin innermost tube and carbon nanowire*

HRTEM micrographs of each MWNT produced by the hydrogen arc evaporation of a pure graphite rod showed highly crystallized walls and a very thin innermost tube.[8] The innermost tube with a diameter of 0.4 nm was the smallest nanotube[8] observed until 2000.

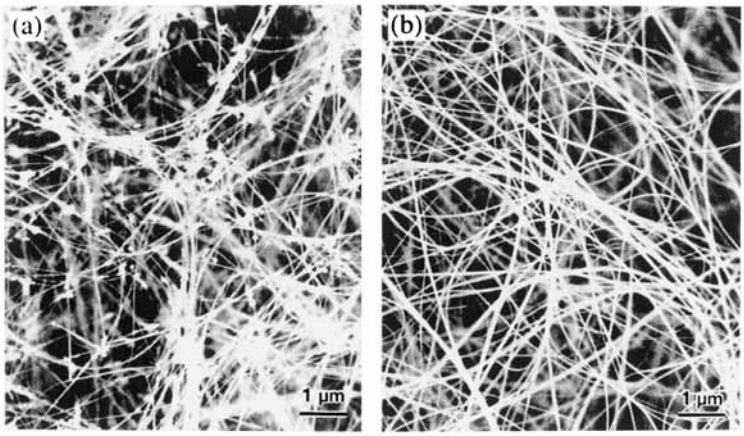

Fig. 7. SEM micrographs of top of cathode deposit.[27] (a) The raw deposit was produced by H_2 (7.98×10^3 Pa) arc evaporation, and the SEM micrograph was obtained in region A (Fig. 6). (b) The same specimen of (a) was heat-irradiated with infrared radiation at 500°C for 30 min.

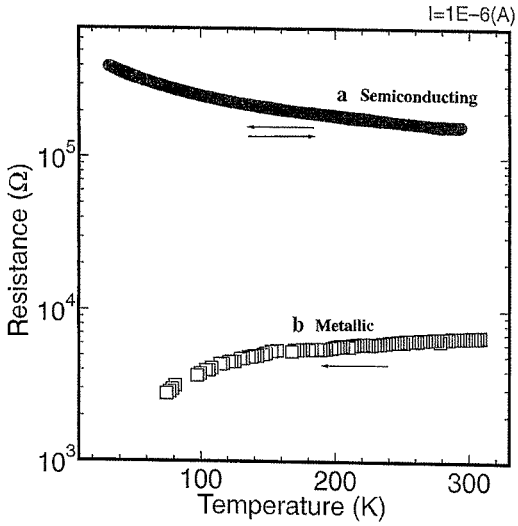

Fig. 8. Temperature dependence[32] of electrical resistance of MWNTs.

However, a 0.3 nm innermost tube was later found,[9] as shown in Fig. 9. Note that the normal distance of MWNT layers is 0.34 nm (similar to the graphite 002 spacing). It is suggested that the 0.4 nm tube has an 'armchair' (3,3) structure and is capped with a C_{20} dodecahedron.[33] For the 0.3 nm tube, chiral index (2,2) and a C_{12} cap are assigned, and energetic calculation is also reported.[9]

In another thin innermost tube, a black line contrast similar to the line contrast of an MWNT was observed[34] at the center of the MWNT, as shown in Figs. 10(a) and 10(b). The center line contrast was observed in the innermost tube with a diameter of 0.7 nm. The tube is capped with a C_{60} hemisphere, as shown in Fig. 10(b). The line contrast is supposed to be the C-chain inserted in the innermost tube of the MWNT with a diameter of 0.7 nm. The MWNT with the carbon chain is considered a new material and named the 'carbon nanowire.' The structure model[34] of this carbon nanowire is shown in Fig. 11.

3.3 *Raman spectra*

The Raman spectra[35,36] of MWNTs produced by hydrogen arc discharge have particular features, as shown in Figs. 12(a) and 12(b). These spectra were obtained by the excitation of an Ar^+ laser (514.5 nm, 2.41 eV). For comparison, the Raman spectra of highly oriented pyrolytic graphite (HOPG) and SWNTs are also shown in the same figure. In the low-frequency region (Fig. 12(a)), many peaks are observed[35] in the case of MWNTs. On the basis of the polarized Raman spectra of oriented MWNTs, the Raman peaks observed in the low-frequency region were confirmed to be the radial breathing modes (RBMs) of thin tubes. The RBM frequency $\omega(\mathrm{cm}^{-1})$ is inversely proportional to the tube diameter d (nm) as presented by the relation[37] $d = 223.75/\omega$. The RBM peak at 570 cm^{-1} in Fig. 12(a) is assigned to that of the thin innermost tube of 0.4 nm. Many RBMs with frequencies higher than those of SWNTs are observed in MWNTs, indicating that the innermost tubes of MWNTs are thinner than those of SWNTs. In the high-frequency region (Fig. 12(b)), a

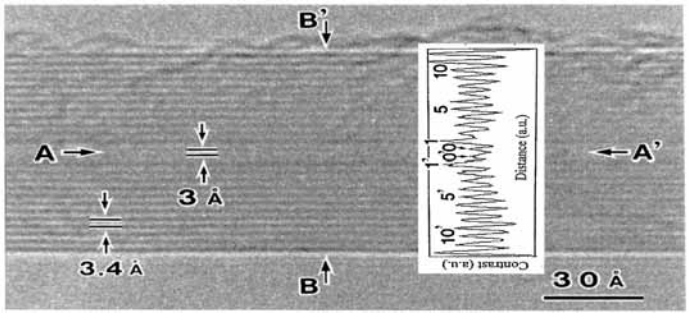

Fig. 9. HRTEM micrograph of MWNT having thinnest innermost tube of 0.30 nm.[9] The inserted densitometer graph is in arbitrary units.

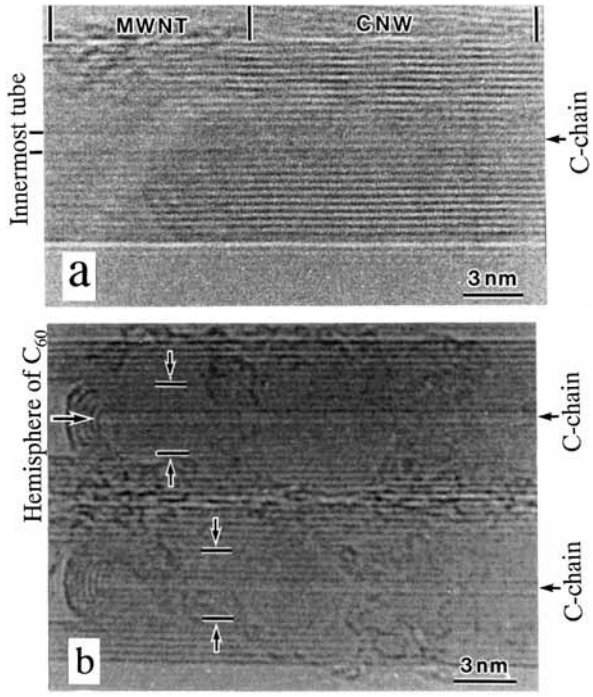

Fig. 10. HRTEM micrographs of carbon nanowire wherein linear C-chain exists in center of MWNT.[34] Different examples of HRTEM micrographs showing C-chain, (a) and (b).

strong *G*-band peak and various splitting peaks are observed.[36] The splitting depends on the chirality of thin nanotubes, metallic or semiconducting. This was confirmed by surface-enhanced Raman spectra obtained from individual MWNTs.

New Raman peaks near 1850 cm^{-1} are observed in MWNTs produced by the hydrogen arc discharge method. The appearance of these new peaks strongly depends on the type of specimen[38,39] and excitation laser energy.[40] The former specimen dependences of these

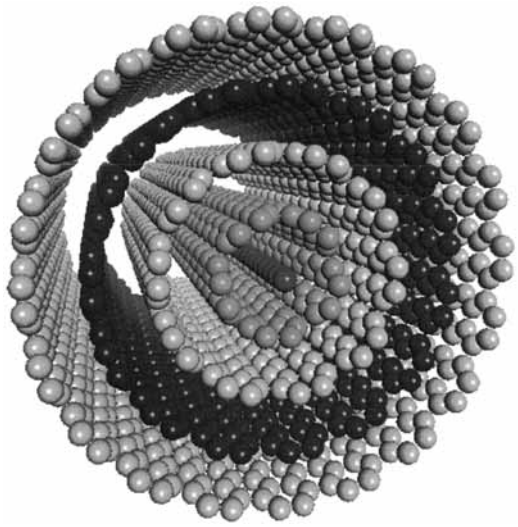

Fig. 11. Atomic model of carbon nanowire.[34] Corresponding TEM micrographs are shown in Figs. 10(a) and 10(b).

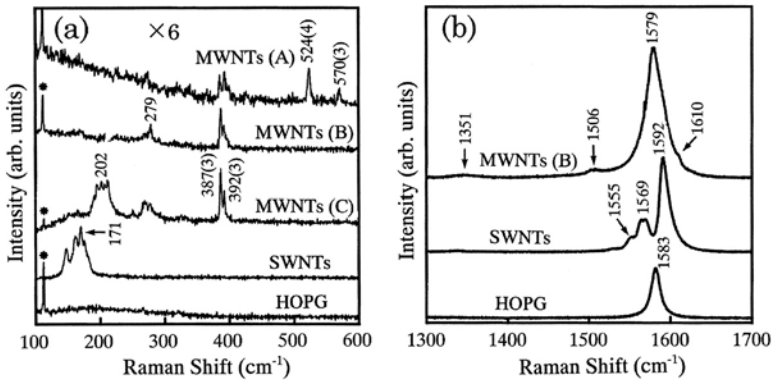

Fig. 12. Raman spectra of MWNTs, SWNTs and HOPG obtained by 514.5 nm excitation.[35,36] (a) Low-frequency region. (b) High-frequency region.

new peaks were clarified by Jinno *et al*.[39] It was confirmed that these new peaks are not associated with hydrogen-based vibrations by comparing the Raman spectra of MWNTs produced in H_2 and D_2 gases. The latter dependence is known as the resonance Raman effect,[40] as shown in Fig. 13. The resonance is marked at the excitations of 2.41 and 2.54 eV.

4. SWNTs Produced by Arc Discharge

4.1 *Production of SWNTs*

Two years after the discovery of MWNTs in 1993, SWNTs were discovered by two groups[10,11] independently. They were produced in the process of metallofullerene produc-

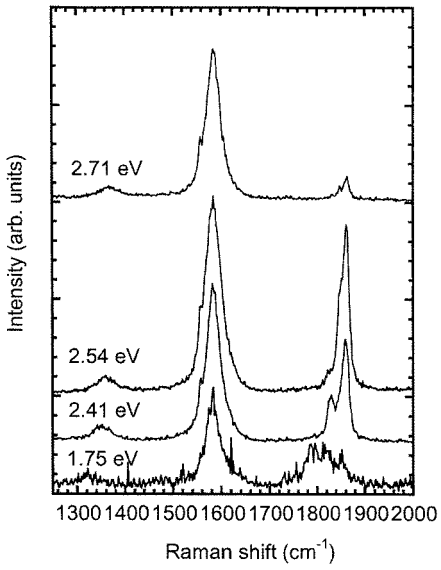

Fig. 13. Resonance Raman spectra[40] of *G*-band peak and new peaks at approximately 1850 cm^{-1}.

tion.[41] Iijima and Ichihashi used a graphite rod including an Fe catalyst,[10] and an IBM group used a graphite rod including a Co catalyst.[11] By the arc discharge evaporation of these graphite rods including a magnetic metal catalyst, SWNTs were produced as cottonlike soot in the chamber, not in the cathode deposit as in the case of MWNTs. Thus, the essential difference between SWNTs and MWNTs is that the former require a catalyst, whereas the latter do not. Moreover, SWNTs are produced in the entire chamber, whereas MWNT production is confined to the cathode deposit. From the latter difference, SWNTs can also be produced by an ac arc discharge method.[42]

The mass production of SWNTs by arc discharge evaporation was first achieved by Journet *et al*.[12] using binary metals, Ni and Y, in He ambient. The present authors[13] modified this method by rearranging the electrodes at a sharp angle of approximately 30°, as shown schematically in Fig. 14. We called it the arc-plasma-jet (APJ) method, and the production rate of the cottonlike soot was increased by this method, as shown in Fig. 15. In the case of using a conventional arc method, more than half of the evaporated anode becomes a cathode deposit, which does not include SWNTs. In contrast, although the evaporation rate is decreased by the APJ method compared with that obtained by the conventional arc method, more than 80% of the evaporated anode becomes soot including SWNTs. When the soot is observed by HRTEM, bundles of SWNTs and catalytic metal particles of Ni surrounded by thick amorphous carbon are observed. The removal of the thick amorphous carbon from the SWNTs is not so easy; when we attempted it by heat treatment, the SWNTs were severely damaged.

4.2 *Macroscopic net of SWNTs produced by arc discharge evaporation*

For an easy purification of SWNTs, the type of catalyst and combinations of ambient gas were considered. For the reduction of amorphous carbon, hydrogen gas and an Fe catalyst

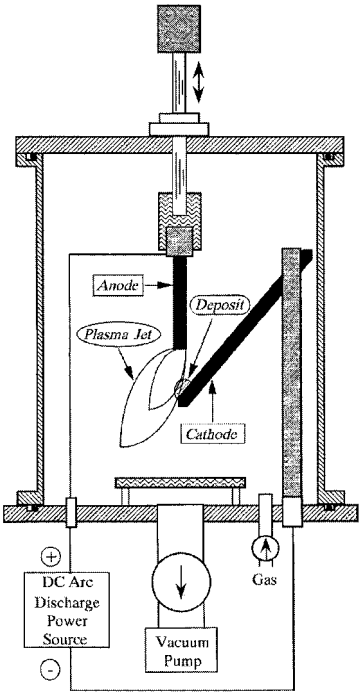

Fig. 14. Schematic diagram of APJ apparatus.[13]

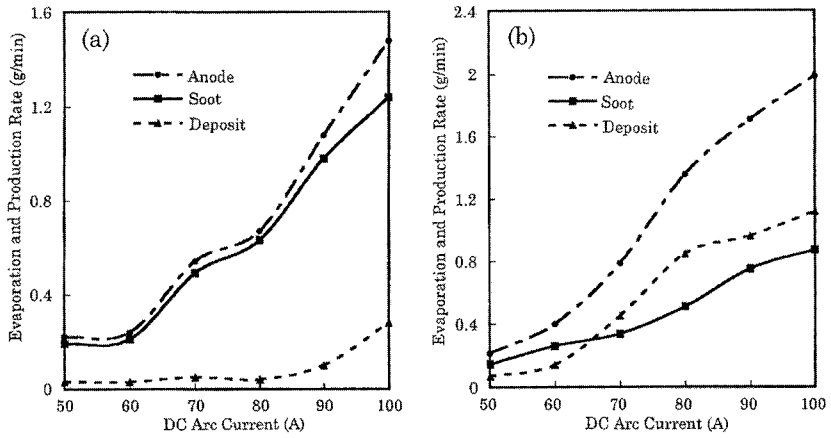

Fig. 15. Evaporation rate of anode, production rate of cottonlike carbon soot, and production rate of deposit measured in SWNT production experiments in He gas of 6.65×10^4 Pa. (a) APJ method.[13] (b) Conventional arc method.

were effective.[14] We call this arc method using Fe and hydrogen ambient the 'FH-arc' method. To stabilize the arc discharge, inert gas was added to the hydrogen gas.[14,43] By the dc arc evaporation of a graphite rod including 1.0 at% Fe in a H_2-Ar gas mixture[14] or H_2-

N_2 gas mixture,[43] the net of SWNTs appeared like a cotton cake. An example of the macroscopic nets of SWNTs produced by the FH-arc method is shown in the optical image[43] in Fig. 16. The SWNT net is longer than 20 cm. When we placed the SWNT net in a 1-liter bottle,[44] the mass was only 1 g, that is, it had a very low green density, approximately 0.001 g/cm^3.

TEM and HRTEM micrographs of the as-grown SWNTs produced by the FH-arc method are shown in Figs. 17(a) and 17(b). The black particles observed in Fig. 17(a) are catalytic Fe particles, which are surrounded by a thin amorphous carbon layer of less than 3 nm, as observed in Fig. 17(b). Therefore, the removal of amorphous carbon by thermal heating in air at 400°C is easy, and bare or oxidized Fe particles can be removed with HCl acid. SEM and TEM micrographs of such purified SWNTs are shown in Figs. 17(c) and 17(d).

5. Other Considerations in Arc-Grown CNTs

By the arc discharge evaporation of graphite rods including rare-earth metals, metallofullerene was produced.[41] The same rare-earth metals were effective in increasing the production of MWNTs.[45,46] On the other hand, SWNTs were produced using graphite rods including different catalytic metals, such as the magnetic metals Fe, Co and Ni, and their mixtures. The latter metals are not effective in producing metallofullerene. This suggests that the growth mechanisms of metallofullerene and SWNTs are different.

By dc arc discharge evaporation in H_2 gas added with 1% H_2S gas,[47] the simultaneous use of many catalysts, namely, Fe, Ni and Co, led to the production of thick SWNTs. In some cases, thick SWNTs included amorphous carbon inside their tubes,[47] and the included amorphous carbon formed incomplete inner tubes. This may correspond to a formation mechanism of double-walled carbon nanotubes (DWNTs). In other cases involving the same specimens, clear DWNTs were also found.[47]

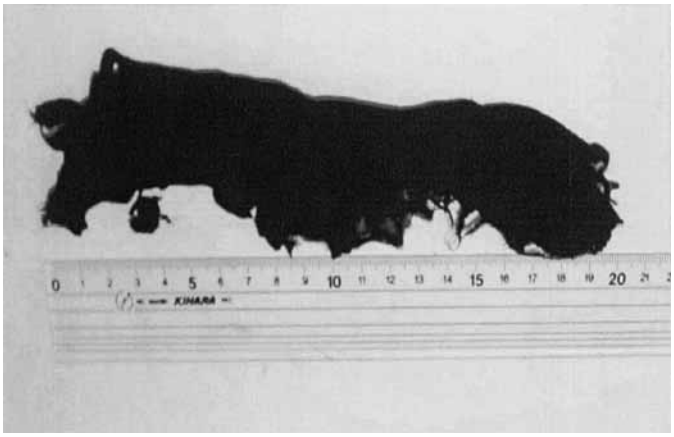

Fig. 16. Macroscopic net of SWNTs produced by dc arc discharge (FH-arc) in H_2-N_2 mixed gas with Fe catalyst.[43]

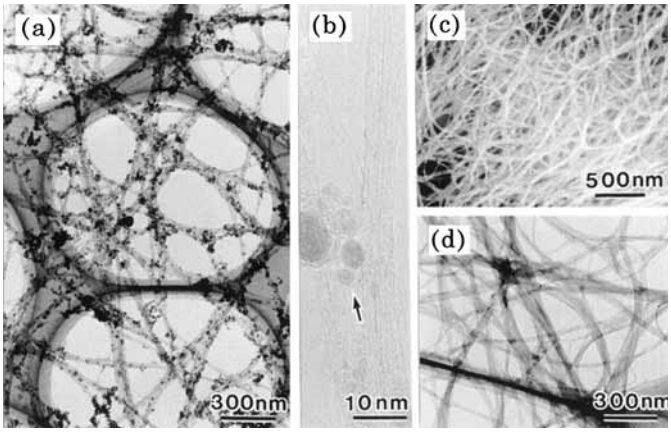

Fig. 17. (a) Low-magnification TEM micrograph of as-grown SWNTs produced by FH-arc method.[14] (b) HRTEM micrograph of as-grown SWNTs. (c) SEM micrograph of purified SWNTs. (d) TEM micrograph of purified SWNT.

The selective production of DWNTs by the arc discharge method has been performed by several groups.[48–50] Sugai *et al*.[50] attempted DWNT production by high-temperature pulse arc discharge. In their case also, thick SWNT and DWNT production conditions were similar.

The modification[51] of the arc discharge method is useful for the semicontinuous synthesis of CNTs. High-purity CNTs were produced by a thermal plasma jet.[52] Arc discharge in liquid,[53] such as water or liquid nitrogen, is also effective for the production of pure CNTs.

6. Conclusion

After the achievement of the mass production of fullerene,[6] arc discharge evaporation was applied to the production of CNTs, namely, MWNTs and SWNTs. In the production of CNTs, three methods, namely, arc discharge, laser ablation and chemical vapor deposition (CVD), were used.[54] It is generally believed that high-crystallinity CNTs can be obtained by laser ablation and arc discharge, but the mass production of CNTs is easy by CVD. In this review, MWNT production by the hydrogen arc discharge method and SWNT production in hydrogen-mixed gases are described. In these production processes, the optical emission spectrum analysis of ambient gas is also important for recognizing growth units.[55,56]

High-crystallinity MWNTs produced by the hydrogen arc discharge method are expected to be used as field emitters with high-current densities at sustainably high voltages. Owing to their high mechanical strength, they may be used as strong and sharp tips for atomic force microscopy. Mass-produced SWNTs by the APJ method are expected to be applied as composite materials owing to their high electric conductivities. Macroscopic SWNT nets produced by FH-arc method are also applied to some composites owing to their superior electric and mechanical properties.

Acknowledgements

The authors thank Dr. Masato Ohkohchi, Dr. Mineo Hiramatsu, Dr. Mukul Kumar and Mr. Sakae Inoue of Meijo University for the discussion and preparation of data.

References

1) S. Iijima: Nature **354** (1991) 56.
2) Y. Ando and M. Ohkohchi: J. Cryst. Growth **60** (1982) 147.
3) R. Uyeda: J. Cryst. Growth **45** (1978) 485.
4) Y. Ando and S. Iijima: Jpn. J. Appl. Phys. **32** (1993) L107.
5) Y. Saito, M. Inagaki, H. Shinohara, H. Nagashima, M. Ohkohchi and Y. Ando: Chem. Phys. Lett. **200** (1992) 643.
6) W. Krätschmer, L. D. Lamb, K. Fostiropoulos and D. R. Huffman: Nature **347** (1990) 354.
7) Y. Saito, N. Suzuki, H. Shinohara and Y. Ando: Jpn. J. Appl. Phys. **30** (1991) 2857.
8) L. C. Qin, X. Zhao, K. Hirahara, Y. Miyamoto, Y. Ando and S. Iijima: Nature **408** (2000) 50.
9) X. Zhao, Y. Liu, S. Inoue, T. Suzuki, R. O. Jones and Y. Ando: Phys. Rev. Lett. **92** (2004) 125502.
10) S. Iijima and T. Ichihashi: Nature **363** (1993) 603.
11) D. S. Bethune, C. H. Kiang, M. S. de Vries, G. Gorman, R. Savoy, J. Vazquez and R. Beyers: Nature **363** (1993) 605.
12) C. Journet, W. K. Maser, P. Bernier, A. Loiseau, M. L. de la Chapelle, S. Lefrant, P. Deniard, R. Lee and J. E. Fisher: Nature **388** (1997) 756.
13) Y. Ando, X. Zhao, K. Hirahara, K. Suenaga, S. Bandow and S. Iijima: Chem. Phys. Lett. **323** (2000) 580.
14) X. Zhao, S. Inoue, M. Jinno, T. Suzuki and Y. Ando: Chem. Phys. Lett. **373** (2003) 266.
15) Y. Ando: *Encyclopedia of Nanoscience and Nanotechnology* Ed. H. S. Nalwa, **1** (2004) 603.
16) Y. Ando, X. Zhao, T. Sugai and M. Kumar: Materials Today **7** (2004) 22.
17) X. Zhao, M. Wang, M. Ohkohchi and Y. Ando: Bull. Res. Inst. Meijo Univ. **1** (1996) 7.
18) T. W. Ebbesen and P. M. Ajayan: Nature **358** (1992) 320.
19) Y. Ando: Fullerene Sci. & Tech. **2** (1994) 173.
20) Y. Tai, K. Inukai, T. Osaki, M. Tazawa, J. Murakami, S. Tanemura and Y. Ando: Chem. Phys. Lett. **224** (1994) 118.
21) M. Wang, X. Zhao, M. Ohkohchi and Y. Ando: Fullerene Sci. & Tech. **4** (1996) 1027.
22) Y. Ando, X. Zhao and M. Ohkohchi: Carbon **35** (1997) 153.
23) X. Zhao, M. Ohkohchi, M. Wang, S. Iijima, T. Ichihashi and Y. Ando: Carbon **35** (1997) 775.
24) X. Zhao, M. Ohkohchi, H. Shimoyama and Y. Ando: J. Cryst. Growth **198/199** (1999) 934.
25) Y. H. Wu, P. W. Qiao, T. C. Chong and Z. X. Shen: Adv. Mater. **14** (2002) 64.
26) M. Hiramatsu, K. Shiji, H. Amano and M. Hori: Appl. Phys. Lett. **23** (2004) 4708.
27) Y. Ando, X. Zhao and M. Ohkohchi: Jpn. J. Appl. Phys. **37** (1998) L61.
28) Y. Ando, X. Zhao and M. Ohkohchi: Jpn. J. Appl. Phys. **37** (1998) 4846.
29) S. Bandow, S. Asaka, X. Zhao and Y. Ando: Appl. Phys. A **67** (1998) 23.
30) Y. Ando, X. Zhao, H. Shimoyama, G. Sakai and K. Kaneto: J. Inorg. Mater. **1** (1999) 77.
31) K. Kaneto, M. Tsuruta, G. Sakai, X. Zhao and Y. Ando: Synth. Met. **103** (1999) 2543.
32) Y. Ando, X. Zhao, H. Kataura, Y. Achiba, K. Kaneto, M. Tsuruta, S. Uemura and S. Iijima: Diamond Relat. Mater. **9** (2000) 847.
33) L.-C. Qin, X. Zhao, K. Hirahara, Y. Ando and S. Iijima: Chem. Phys. Lett. **349** (2001) 389.
34) X. Zhao, Y. Ando, Y. Liu, M. Jinno and T. Suzuki: Phys. Rev. Lett. **90** (2003) 187401.
35) X. Zhao, Y. Ando, L.-C. Qin, H. Kataura, Y. Maniwa and R. Saito: Chem. Phys. Lett. **361** (2002) 169.

36) X. Zhao, Y. Ando, L.-C. Qin, H. Kataura, Y. Maniwa and R. Saito: Appl. Phys. Lett. **81** (2002) 2550.
37) S. Bandow, S. Asaka, Y. Saito, A. M. Rao, L. Grigorian, E. Richter and P. C. Eklund: Phys. Rev. Lett. **80** (1998) 3779.
38) Y. Ando, X. Zhao, H. Kataura, Y. Achiba, K. Kaneto, S. Uemura and S. Iijima: Trans. Mater. Res. Soc. Japan **25** (2000) 817.
39) M. Jinno, S. Bandow and Y. Ando: Chem. Phys. Lett. **398** (2004) 256.
40) H. Kataura, Y. Kumazawa, N. Kojima, Y. Maniwa, I. Umezu, S. Masubuchi, S. Kazama, X. Zhao, Y. Ando, Y. Ohtsuka, S. Suzuki and Y. Achiba: *AIP Conference Proceedings* **486** (1999) 328.
41) H. Shinohara, H. Sato, M. Ohkohchi, Y. Ando, T. Kodama, T. Shida, T. Kato and Y. Saito: Nature **357** (1992) 52.
42) M. Ohkohchi: Jpn. J. Appl. Phys. **38** (1999) 4158.
43) Y. Ando, X. Zhao, S. Inoue, T. Suzuki and T. Kadoya: Diamond Relat. Mater. **14** (2005) 729.
44) Y. Ando, X. Zhao, S. Inoue, T. Suzuki, M. Ohkohchi and T. Kadoya: Trans. Mater. Res. Soc. Japan **30** (2005) 1193.
45) M. Ohkohchi, Y. Ando, S. Bandow and Y. Saito: Jpn. J. Appl. Phys. **32** (1993) L1248.
46) M. Ohkohchi, X. Zhao, M. Wang and Y. Ando: Fullerene Sci. & Tech. **4** (1996) 977.
47) Y. Ando, X. Zhao, K. Hirahara and S. Iijima: Am. Inst. Phys., CP590, *Nanonetwork Materials*, (2001) 7.
48) J. L. Hutchison, N. A. Kiselev, E. P. Krinichnaya, A. V. Krestinin, R. O. Loutfy, A. P. Morawsky, V. E. Muradyan, E. D. Obraztsova, J. Sloan, S. V. Terekhov and D. N. Zakharov: Carbon **39** (2001) 761.
49) Y. Saito, T. Nakahira and S. Uemura: J. Phys. Chem. B **107** (2003) 931.
50) T. Sugai, H. Yoshida, T. Shimada, T. Okazaki, S. Bandow and H. Shinohara: Nano Lett. **3** (2003) 769.
51) C. Liu, H. T. Cong, F. Li, P. H. Tan, H. M. Cheng, K. Lu and B. L. Zhou: Carbon **37** (1999) 1865.
52) J. Hahn, J. H. Han, J.-E. Yoo, H. Y. Jung and J. S. Suh: Carbon **42** (2004) 877.
53) N. Sano, H. Wang, M. Chhowalla, I. Alexandrou and G. A. J. Amaratunga: Nature **414** (2001) 506.
54) M. Terrones: Internat. Mater. Rev. **49** (2004) 325.
55) X. Zhao, T. Okazaki, A. Kasuya, H. Shimoyama and Y. Ando: Jpn. J. Appl. Phys. **38** (1999) 6014.
56) Y. Guo, T. Okazaki, T. Kadoya, T. Suzuki and Y. Ando: Diamond Relat. Mater. **14** (2005) 887.